Available online at www.sciencedirect.com
SCIENCE DIRECT
Cement and Concrete Research 35 (2005) 1385–1390
Cement and Concrete Research

# Online SEM investigation of microcrack characteristics of concretes at various temperatures

Xi-Shu Wang[a,*], Bi-Sheng Wu[a], Qing-Yuan Wang[b]

[a]Department of Engineering Mechanics, School of Aerospace, Tsinghua University, Beijing 100084, PR China
[b]Department of Civil Engineering and Mechanics, Sichuan University, Chengdu 610065, PR China

Received 19 September 2003; accepted 12 July 2004

**Abstract**

Detecting and quantifying microcracking damage in microscopy has become an integral aspect of concrete technology. Better methods that have emerged over the last decade have led to improved understanding of the failure mechanisms and consequent effect on mechanical properties of concretes. This paper focuses on the applications of the scanning electron microscope (SEM) in situ observations of concrete and the description of their microcrack characteristics at different temperatures. For the sake of brevity, nondestructive evaluations of large-scale cracking, such as delaminations and spalling, have not been addressed here. The microcracks propagation is a critical factor at high temperatures. These results indicated that the thermal energy plays an important role in microcracking and propagation of these concretes and reflected that there are different fracture types with changing the microstructure of concretes. The thermal mismatch of mixed materials play a significant role in the microcracking damage of concrete.


*Keywords:* High-performance concrete; Temperature; Characterization; Microcracking; SEM

## 1. Introduction

Researchers working with concrete and cement became interested in Griffith's theory of fracture in the late 1950s. Very soon, it was evident that the classical fracture mechanics parameters, such as the energy release rate $G_c$ or the stress intensity factor $K_{IC}$, seem to depend on both the specimen size and the types of loading. By the mid 1960s, it was quite evident that even under the simplest tensile loading, a multitude of microcracking and other nonlinear phenomena were responsible for the deviations of concrete's fracture behavior from predictions of linear elastic fracture mechanics theory [1–3]. The following three decades saw an extensive research effort aimed at understanding and modeling these nonlinear phenomena of concretes. These studies evolved into two distinct approaches towards modeling nonlinearity. The first, based on a smeared crack approach [4,5], involved a diffuse zone of microcracks and damage-based constitutive modeling. The second involved localized crack and ligament connections for continued transfer of stress cross the crack [6], e.g., the "fictitious crack model". Irrespective of their nature, the validation and calibration of these models made it essential to improve the detection and measurement of failure/fracture under different testing conditions. However, more advanced processing techniques and methods of predicting mechanical/failure behavior in microscopy related to durability and toughness continuously to be explored [7]. Employing experimental technique to monitor the initiation and propagation of microcrack is a critical step in the process of developing such as high-performance concrete (HPC). HPC would be required to provide long-term seals for man-made openings and associated disturbed regions, which are often exposed to high temperature and confining pressures [8–11].

Until now, little information has been available on the microcrack initiation and propagation behavior of HPC at

* Corresponding author. Tel.: +86 10 62792972; fax: +86 10 62781824.
*E-mail address:* xshwang@tsinghua.edu.cn (X.-S. Wang).

0008-8846/$ - see front matter © 2004 Elsevier Ltd. All rights reserved.
doi:10.1016/j.cemconres.2004.07.015

high temperature, particularly for HPC, with the incorporation of mineral and arenaceous admixtures [12]. The present study is aimed to characterize microcracking nulceation and evolution for two types of concretes at different temperatures by in situ observations with scanning electron microscope (SEM) and to examine the effect of microstructure and thermal energy on the microcracking of these concretes.

## 2. Materials and experimental procedures

In this study, the concrete mixtures were prepared with Types C (cement paste mortar) and M (mortar intermixed with sands), respectively. Superplasticizer and silica fume were incorporated in the two mixtures, which contained various proportions of fine siliceous components such as fly ash, silica fume and slag. The compositions of the two concretes mixtures are similar to that reported by Li et al. [12]. The two kinds of specimens were fabricated by the Department of Civil Engineering, Hong Kong Institute of Technology. Flat specimens with a 20-mm gage length and a $10\times3.5\text{-mm}^2$ gage cross-section were used for various temperature tests from room temperature up to the maximum 500 °C. All specimens were dried out prior to these tests.

The faces of the samples were carefully prepared by the shadowing casting process in the vacuum chamber (about 30 min) prior to tests to show the microstructure clearly by in situ observation with SEM. All tests were performed in the vacuum chamber of the SEM system using specially designed servo-hydraulic testing system by Shimadzu, which provided not only the static and but also the pulsating (sine wave) loadings at 10 Hz of ±10 kN maximum capacity. The signal of the SEM can be directly transferred to a computer via a direct memory access type A/D converter, making it possible to photo 960×1280 frames of SEM images successively [13–16]. All compressive tests were controlled under a constant loading of about 200 N (about 5.71 MPa). The temperature, controlled using a thermoelectric couple in the small clamber, increased from 25 to 100, 200, 300, 400 and 500 °C in 60 min and then held these values for about 60 min, respectively. The error of the thermal control was less than ±1 °C. Therefore, the samples underwent the thermal–mechanical coupling action although the mechanical loading was small. The compressive loading of about 200 N mainly restricted the loose deformation of the sample at high temperature. To validate the effect of applied mechanical loading on the deformation of specimens, the axial compressive tests for the concretes were carried out with strain gages of 1×1 mm in size at room temperature. The relationships between the stress and strain of samples are shown in Fig. 1. The relations of stress and strain of both types C and M concretes at room temperature are linear when the stress level is lower than 35 MPa. However, as the interstice of the type C concrete is more

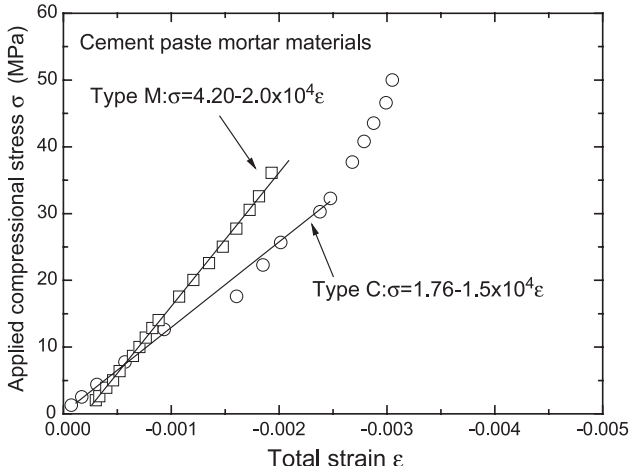


Fig. 1. Stress–strain curve for cement paste mortar at room temperature.

than that of the type M concrete, its deformation is rather larger with increasing the applied loading, the slope of curve of the type M concrete presents precipitous. Generally, the stress–strain relations cannot be obtained from these tests in situ observation with SEM at the high temperature because it is difficult to evaluate the stain in this vacuum chamber of the SEM system. In our experiments, we measured the surface strains in microscopy at high temperature from the in situ SEM images using the Digital Speckle Correlation Method (DSCM). The results will be discussed in the sequel.

For the two types of concretes (types C and M), a considerable difference was found in the compressive elastic moduli, as shown in Fig. 1. This indicates that the deformation capability of type C concrete is higher than that of type M when subjected the applied compressive loading. The curve slopes of the stress–strain curves of the two concretes are approximately identical under lower compressive stress, but the difference in the two curves increases with the increasing applied compressive loading. In addition, the whole process of crack initiation and propagation in the two types of concretes was also monitored or recorded in situ with SEM at high temperature.

## 3. Results and discussions

Fig. 2 serially gives three SEM micrographs of the surface microstructure of concretes of types C and M intermixed with sands. It is clearly seen from Fig. 2(a) and (b) that an abundance of hydrated phases and pores, as well as cores such as $Ca(OH)_2$ dendrite crystals or other crystals (marker “CH”), and intermixed with calcium silicate hydrate (C-S-H; marked “CSH”), as well as granular structure, exists in concrete C. However, concrete M possesses different microstructures, as shown in Fig. 2(c) The microstructures may be characterized in terms of porosity and hydration progress. The two physical mechanisms are obviously linked with each other. Hydration in the vicinity of

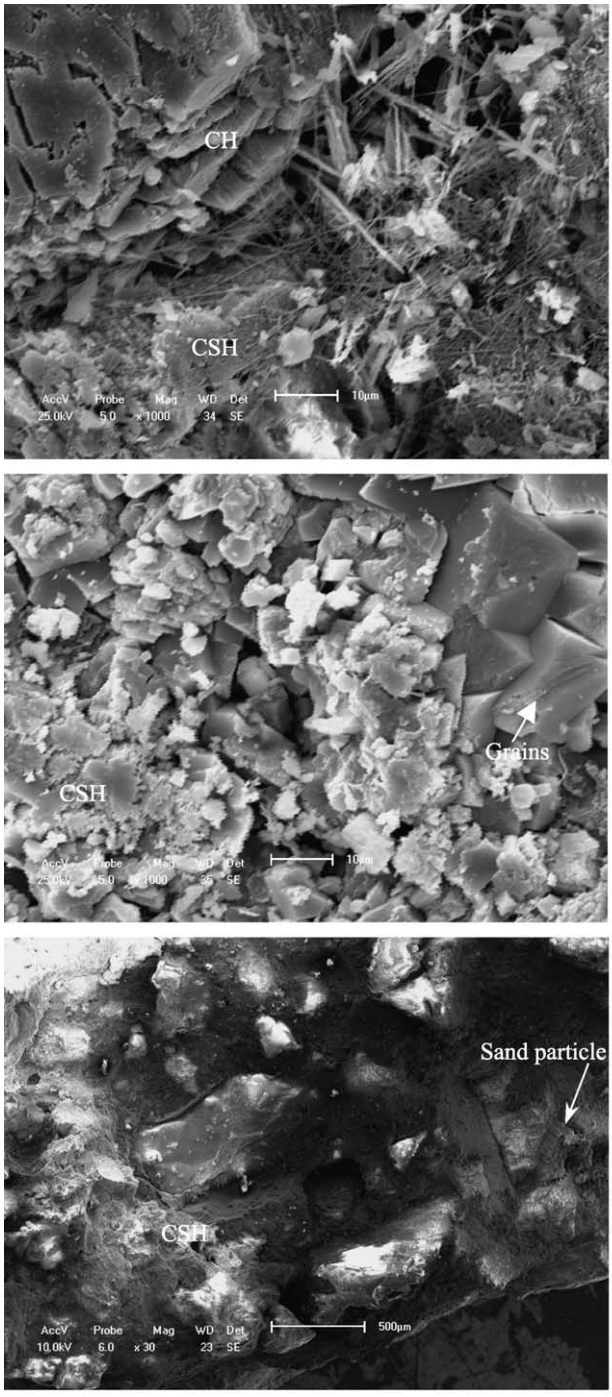


Fig. 2. (a) SEM micrograph of microstructure-hydrated dendrites for type C (scale bar 10 μm). (b) SEM micrograph of microstructure-hydrated grains for type C (scale bar 10 μm). (c) SEM micrograph of surface microstructure for type M (scale bar 500 μm).

aggregate grains differs from the reaction that takes place in the bulk paste because the water/cement (W/C) ratio is locally higher and because the growth and the nature of hydrates may be influenced by the surface and chemical nature of aggregates. Therefore, the excess of porosity is both the cause and the consequence of the existence of interfacial transition zone [17]. Similar findings were

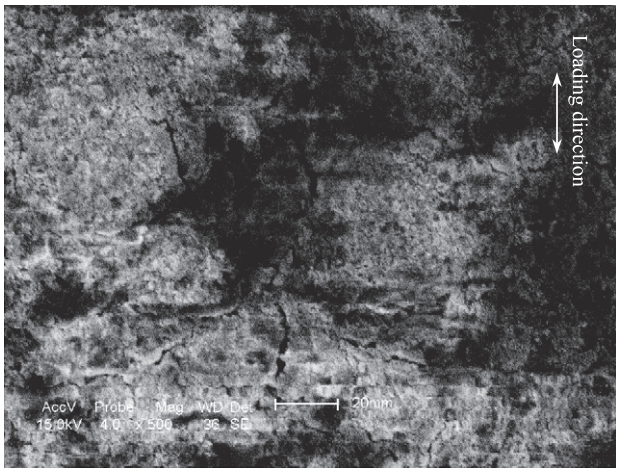


Fig. 3. Surface cracking for the type C after elevating 100 °C holding 60 min (scale bar 20 μm).

reported earlier by Handoo et al. [9] and Sidney [18]. In situ observation with SEM to investigate the surface microstructure of the two types concretes also indicates that the compressible capability of type C was higher than that of type M. Therefore, the difference in the compressive elastic moduli of the two types of concretes (Fig. 1) can be easily understood from their distinctly different microstructure. Theoretical analysis on the dependence of effective elastic moduli of concretes on the microstructures presents an interesting problem in micromechanics [3,19] but is beyond the scope of the present study.

Furthermore, the hardnesses of the two types of concrete depend on their microstructures too. The hardness of type M is higher than that of type C because the microstructure of the former is rather dense. However, their compressible strength depends not only on their hardness but also on their crack initiation and propagation mechanism. Besides the effect of the applied stress on the microcracking of concretes, the temperature environmental plays an important role in the microcracking of concretes.

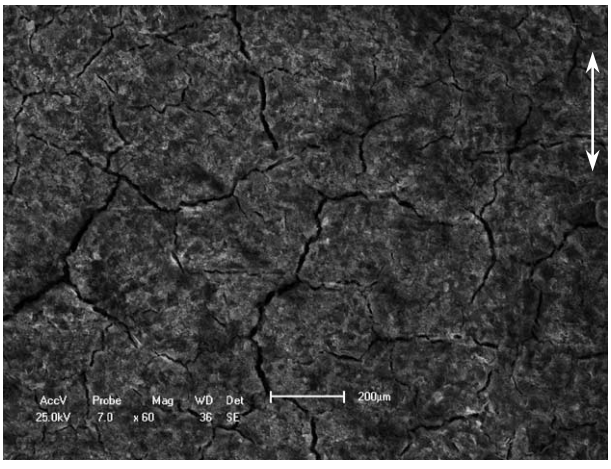


Fig. 4. Surface cracking for the type C after elevating 200 °C holding 60 min (scale bar 200 μm).

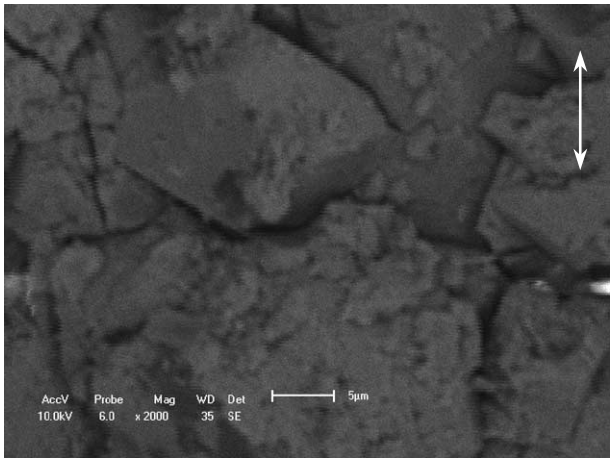


Fig. 5. Surface cracking for the type C after elevating 300 °C holding 60 min (scale bar 5 μm).

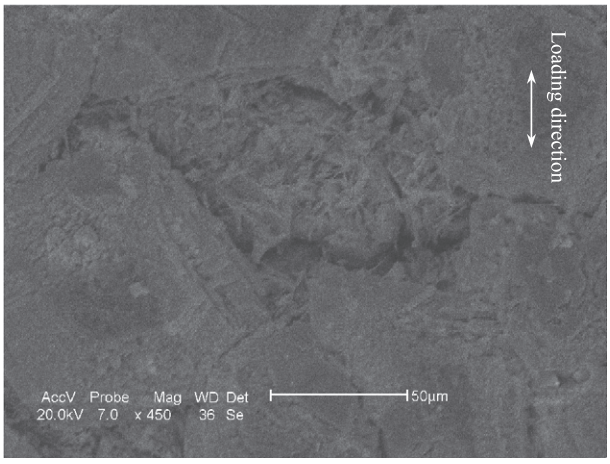


Fig. 7. Surface cracking for the type C after elevating 500 °C holding 60 min (scale bar 50 μm).

A number of SEM micrographs illustrating the microstructure characteristics of the type C concrete at 100, 200, 300, 400 and 500 °C are shown in Figs. 3–7, respectively. These surface micrographs of the samples were taken after elevating up to the maximum temperature and holding for 60 min. Well-developed microcracks along the boundaries of the aggregate particles can be clearly observed from these figures. As the temperature increases, the density of microcracks increases, as can be seen in Figs. 3 and 4. In type C concrete, most microcracks nucleate basically along the applied loading direction. Therefore, the crack opening displacement (COD) in the tension direction is greater than that in the transversal direction [3]. Therefore, brittle failure is one of the typical failure mechanisms of concrete, even at microscopy and at high temperature. The density of cracks increases with the elevating temperature. At the same time, it resulted in the initiation and propagation of microcracks in type C concrete at moderate temperatures. To validate the distinct effect of moderate temperature on microcrack initiation and propagation, the SEM micrographs at different temperatures, from 300 to 500 °C, are shown in Figs. 5–7. The characteristics of microcrack initiation and propagation are similar to those as shown in Figs. 3 and 4. But these microcracks did not continually propagate along the loading direction as the temperature increased. One of the main reasons is that the intermixture with C-S-H becomes soft and enhanced adhesion between the intermixed and hydrated phases at moderate temperature, then causes some microcracks to be closed at the boundaries. These micrographs indicated that the important characteristic is that the microcracks of type C concrete deformed between about 100 and 200 °C. However, this did not lead to the cleavage failure of aggregate particles. It was found that the thermal energy contribution to the microcracks initiation and propagation of type C concrete is mainly in the range of 150–200 °C. This contribution indicated the microcrack initiation mechanism at high temperature, which is as the thermal shrinkage of the matrix of cement paste and the aggregate particles or cement grains misfits or as the local material properties and local temperature gradient are

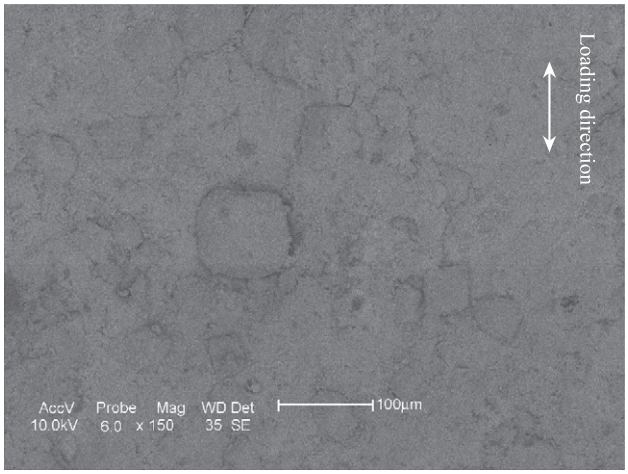


Fig. 6. Surface cracking for the type C after elevating 400 °C holding 60 min (scale bar 100 μm).

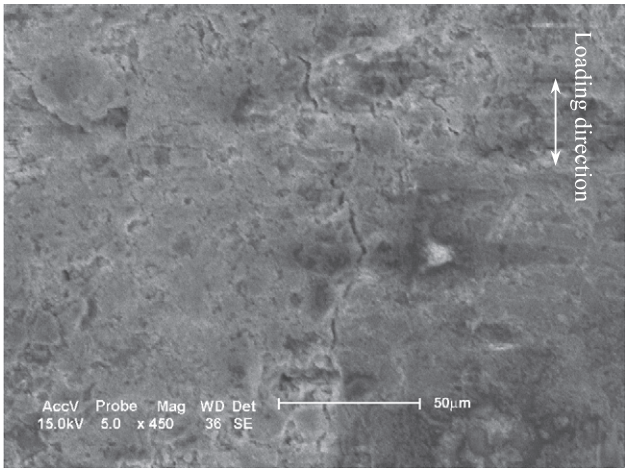


Fig. 8. Surface cracking for the type M after elevating 100 °C holding 60 min (scale bar 50 μm).

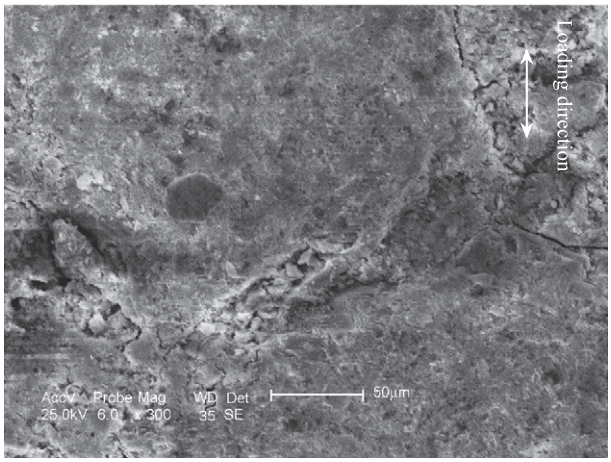


Fig. 9. Surface cracking for the type M after elevating 200 °C holding 60 min (scale bar 50 μm).

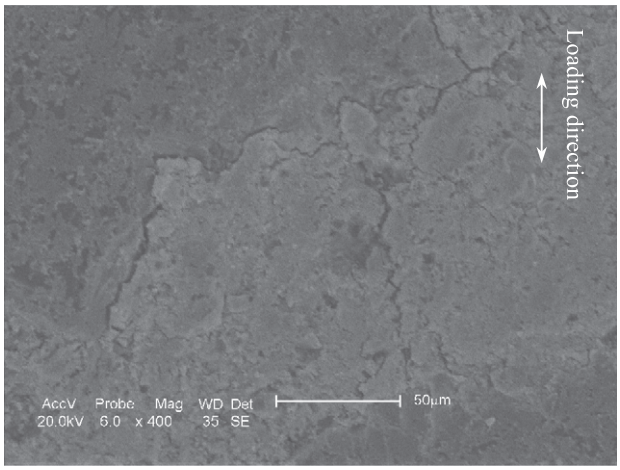


Fig. 11. Surface cracking for the type M after elevating 400 °C holding 60 min (scale bar 50 μm).

different. Therefore, the temperature of about 200 °C may be a critical value for microcracking nucleation in the concretes under service. In addition, the effect of elevating temperature ratio on the microcrack initiation of the concrete is not obvious within 2–8 °C/min. Therefore, the strength of concrete would decrease at high temperature because of microcracking damage evolution, as is different from that of the rock as the structural concrete in civil engineering [20].

SEM micrographs of type M concrete intermixed with the sands at various temperatures, as shown in Figs. 8–12, reveal well-developed microcrack initiation and propagation. Similar analysis of type C concrete was carried out, as shown in Figs. 3–7. It can be also clearly seen that microcracks existed on the surface of type M concrete when the temperature was elevated up to 100 °C, and microcracks propagate mainly along the applied loading direction. Therefore, the microcrack initiation and propagation mechanism of type M concrete is analogous to that of type C concrete. But the density of microcracks for type M concrete is smaller than that for type C concrete at the same temperature. The original crack propagation at the boundaries of aggregate particles is explained by the boundary effect because the shrinkage ratios of both aggregate particles and intermixed are different. Other characteristics of crack initiation and propagation for type M include the following: (1) microcracks generally initiated around the boundary of sands and accompanied the sand to be cleaved, as shown in Fig. 10, and (2) the sensitivity of the elevating temperature ratio to microcracks initiation is not obvious within 2–8 °C/min. This implies that the sand may expand when it undergoes thermal loading and the cement paste mortar shrunk at moderate temperature. Comparing the two types of concretes at different temperatures, microcrack initiation also occurred in type M concrete at temperatures between 100 and 200 °C. At the same time, in situ observation with SEM to microcrack initiation and propagation is limited when the temperature is over 500 °C. That is because the observational surface of the samples is affected by the volatile covering or matter in concrete at temperatures over 500 °C. The fact testifies that

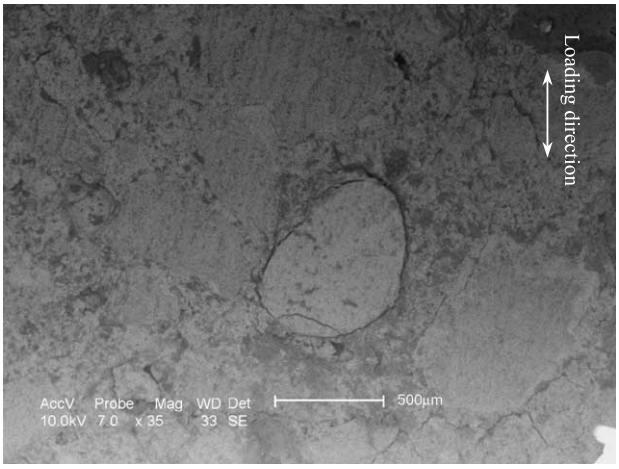


Fig.10. Surface cracking for the type M after elevating 300 °C holding 60 min (scale bar 500 μm).

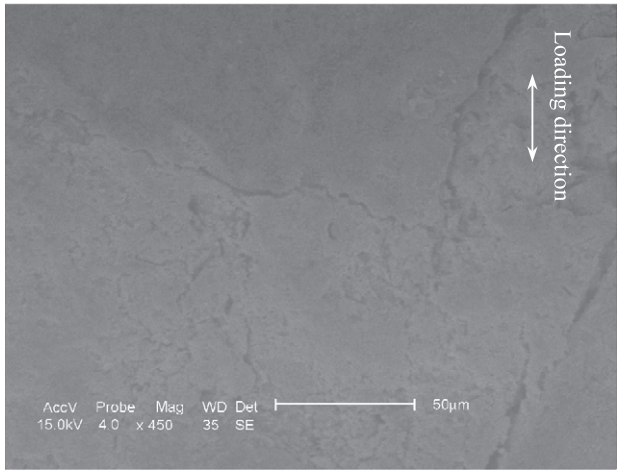


Fig. 12. Surface cracking for the type M after elevating 500 °C holding 60 min (scale bar 50 μm).

the definition of SEM micrographs at over 300 °C is obviously blurrier than that at down 300 °C.

## 4. Conclusions

We have studied, via in situ SEM observations, the characteristics of microcracking damage of concretes of types C and M at different temperatures. The dependence of the macroscopic effective properties and physical mechanisms of damage on microstrucutres have been examined. The main results obtained in this paper are as follows:

1. The mechanical properties of type M concrete (mortar intermixed with sands) are better than those of type C concrete (no intermixed with the sands), not only at room but also at high temperature.
2. Most of nucleated microcracks in cement paste mortar are distributed mainly along the applied loading direction, and the crack opening displacement (COD) in the loading direction is greater than that in the transversal direction. This indicates that their failures are mainly brittle, even at high temperature. At the same time, there are different cracking numbers in the two types of concrete at the same condition. Therefore, it is obvious that the intermixed sand affects not only the microstructure but also the statistical distributions of microcracks.
3. These SEM micrographs indicate the important characteristics that microcracks in type C and type M concretes were deformed at about 200 °C. Although this is not a failure phenomenon of cleaved aggregate particles for type C, there exists a cleaved sand grain for type M concrete. Therefore, the temperature of about 200 °C is a critical value for the concrete under service. In addition, the effect of elevating temperature ratio on the microcrack initiation of the concretes is not obvious within 2–8 °C/min.

## Acknowledgement

The authors would like to thank Professor Xi-Qiao Feng for valuable discussions and gratefully acknowledge the support from the Fracture Mechanics Key Lab of Ministry of Education of China.

## References

[1] J. Glucklich, Jpn. Soc. Strength Fract. Mater. 3 (1966) 1343–1382.
[2] M. Elices, J. Planas, Fracture mechanics parameters of concrete, Adv. Cem. Based Mater. 4 (3–4) (1996) 116–127.
[3] X.Q. Feng, S.W. Yu, Damage Micromechanics of Quasi-Brittle Solids, Higher Education Press, Beijing, 2002.
[4] Z.P. Bazant, B.H. Oh, Crack band theory for fracture of concrete, Mater. Struct. 16 (1983) 155–177.
[5] Z.P. Bazant, E.B. Giraudon, Statistical predication of fracture parameters of concrete and implications for choice of testing standard, Cem. Concr. Res. 32 (2002) 529–556.
[6] A. Hillerborg, M. Modeer, P.E. Petersson, Analysis of crack formation and crack growth in concrete by means of fracture mechanics and finite elements, Cem. Concr. Res. 6 (1976) 773–782.
[7] A.K. Maji, Review of noninvasive techniques for detecting microfracture, Adv. Cem. Based Mater. 2 (1995) 201–209.
[8] S. Ghosh, K.W. Nasser, Effect of high temperature and pressure on strength and elasticity of lignite fly ash and silica fume concrete, ACI Mater. J. 93 (1) (1996) 51–60.
[9] S.K. Handoo, S. Agarwal, S.K. Agarwal, Physicochemical, mineralogical, and morphological characteristics of concrete exposed to elevated temperatures, Cem. Concr. Res. 32 (2002) 1009–1018.
[10] G.C. Mays, Performance requirements for structural adhesives in relation to concrete strengthening, Int. J. Adhes. Adhes. 21 (2001) 423–429.
[11] N. Narayanan, K. Ramamurthy, Structure and properties of aerated concrete: a review, Cem. Concr. Compos. 22 (2000) 321–329.
[12] X.J. Li, Z.J. Li, M. Onofrei, G. ballivy, K.H. Khayat, Microstructural characteristics of HPC under different thermo–mechanical and thermo–hydraulic conditions, Mater. Struct. 32 (1999) 727–733.
[13] X.S. Wang, J.H. Fan, SEM online investigation of fatigue crack initiation and propagation in cast magnesium alloy, J. Mater. Sci. 39 (7) (2004) 2617–2620.
[14] X.S. Wang, X. Lu, H.D. Wang, Investigation of surface fatigue microcrack growth behavior of cast Mg–Al alloy, Mater. Sci. Eng., A Struct. Mater.: Prop. Microstruct. Process. 364 (2004) 11–16.
[15] X.S. Wang, Y. Xu, X.Q. Xu, Direct observations of microcracking in the fuel plate using a scanning electron microscope, Appl. Compos. Mater. 11 (3) (2004) 145–154.
[16] X.S. Wang, Y. Xu, Experiments, characterizations and analysis of a dispersion $U_3Si_2$–Al fuel plate with sandwich structure, J. Nucl. Mater. 328 (2–3) (2004) 243–248.
[17] J.P. Ollivier, J.C. Maso, B. Bourdette, Interfacial transition zone in concrete, Adv. Cem. Based Mater. 2 (1995) 30–38.
[18] D. Sidney, Identification of hydrated cement constituents using a scanning electron microscope-energy dispersive X-ray spectrometer combination, Cem. Concr. Res. 2 (5) (1972) 617–632.
[19] X.Q. Feng, J.Y. Li, S.W. Yu, A simple method for calculating interaction of numerous microcracks and its applications, Int. J. Solids Struct. 40 (2) (2003) 447–464.
[20] T.F. Wang, R.H.C. Wong, M.R. Jiao, K.T. Chau, C.A. Tang, Micromechanics and rock failure process analysis, Key Eng. Mater. 261–263 (2004) 39–44.